Theor Chem Acc (2011) 129:85–92
DOI 10.1007/s00214-011-0896-x

REGULAR ARTICLE

Theoretical study of phenol adsorption on the (8, 0) silicon carbide nanotube

Jing-xiang Zhao · Bo Gao · Qing-hai Cai · Xiao-guang Wang · Xuan-zhang Wang

Received: 18 November 2010 / Accepted: 19 January 2011 / Published online: 16 February 2011

Abstract Phenol adsorptions on solid surfaces have attracted considerable attention due to their potential applications. Through density functional theory (DFT) methods, we study phenol adsorption on a semiconducting (8, 0) silicon carbide nanotube (SiCNT). We find that the hydroxyl group of phenol prefers to attach to the Si atom of SiCNT. The calculated adsorption energy is −0.494 eV, and 0.208 electrons are transferred from the adsorbate to the nanotube. Interestingly, the O–H bond of the adsorbed phenol can be split on the SiCNT, in which the H atom of the O–H group in the phenol is transferred from the Si atom to its neighboring C atom. Furthermore, we also explore the π–π interaction between the aromatic ring of the phenol and the hexagons of the SiCNT. The calculated adsorption energy is about −0.285 eV with a neglectable charge transfer (0.064 e). On the basis of the calculated band structures, we find that the electronic properties of the adsorbed SiCNT by the phenol are little changed. The present results might be helpful not only to provide an effective way to convert or remove phenol but also to widen the application fields of the SiCNT.

Keywords Silicon carbide nanotube · Phenol · Adsorption · Density functional theory

Electronic supplementary material The online version of this article (doi:10.1007/s00214-011-0896-x) contains supplementary material, which is available to authorized users.

J. Zhao (✉) · B. Gao · Q. Cai · Xiao-guang Wang · Xuan-zhang Wang
College of Chemistry and Chemical Engineering and Provincial Key Lab for Advanced Functional Materials and Excite State, Harbin Normal University, 150025 Harbin, People's Republic of China
e-mail: xjz_hmily@yahoo.com.cn

1 Introduction

The adsorptions of simple organic molecules on solid surfaces have been long studied [1–3]. Particularly, phenol adsorptions on metal and semiconductor surfaces have attracted considerable attention recently [4–27]. This is because: (a) phenol may be involved in some stepwise reactions, where the molecule anchors to the surface with one functional group in the first step, followed by the interaction with an incoming reactant [14–20]. In other words, phenol adsorption is a key step toward the initiation of many catalytic reactions, thereby leading to the formation of a variety of products, such as bisphenol, phenolic resins, caprolactam, aniline, and alkylphenols [21]; (b) Phenol appears as a side group in amino acid tyrosine, thus it is relevant to protein folding and protein adsorption [22]. Moreover, phenol also exists as an end or side group of some polymers, therefore likewise playing an active role in the polymer adhesion processes. This property of the phenol renders it potential for developing organic opo-electronic devices, molecular-scale electronics, biofunctionality, and novel hybrid materials [23–26]; (c) Phenol is a toxic byproduct in industrial processes and can cause serious impairment to human health. Thus, removing phenol from water or gaseous streams is highly desirable from environmental perspectives [27].

In view of the aforementioned potential applications of the phenol as well as its toxicity, there have been many studies on phenol adsorption on solid surfaces [4–35]. For example, through reflection–adsorption infrared spectroscopy (RAIS) and Auger electron spectroscopy, Myers and co-workers have studied the interaction of the phenol with the Ni (111) surface experimentally [20]. Xu and Ihm have independently shown that the O–H bond of the phenol can be effectively split on Rh and Pt surfaces in experiment [14, 15].

Theoretically, by comparing several different adsorption sites and orientations, Delle Site et al. have found that phenol adsorption at the bridge site of the Ni (111) surface is the most energetically favorable [28]. Furthermore, they have investigated the cleavage of O–H bond of phenol on different Ni surfaces [29]. Additionally, phenol adsorption on Au [30] and Al [31] surfaces have also been reported. Adsorption of phenol on semiconducting surfaces provides a potential way to produce smaller transistors [1–5]. While there have been many studies concerning adsorption of phenol molecule on metal surfaces, there are surprisingly few studies concerning phenol adsorption on semiconducting surfaces [32–35].

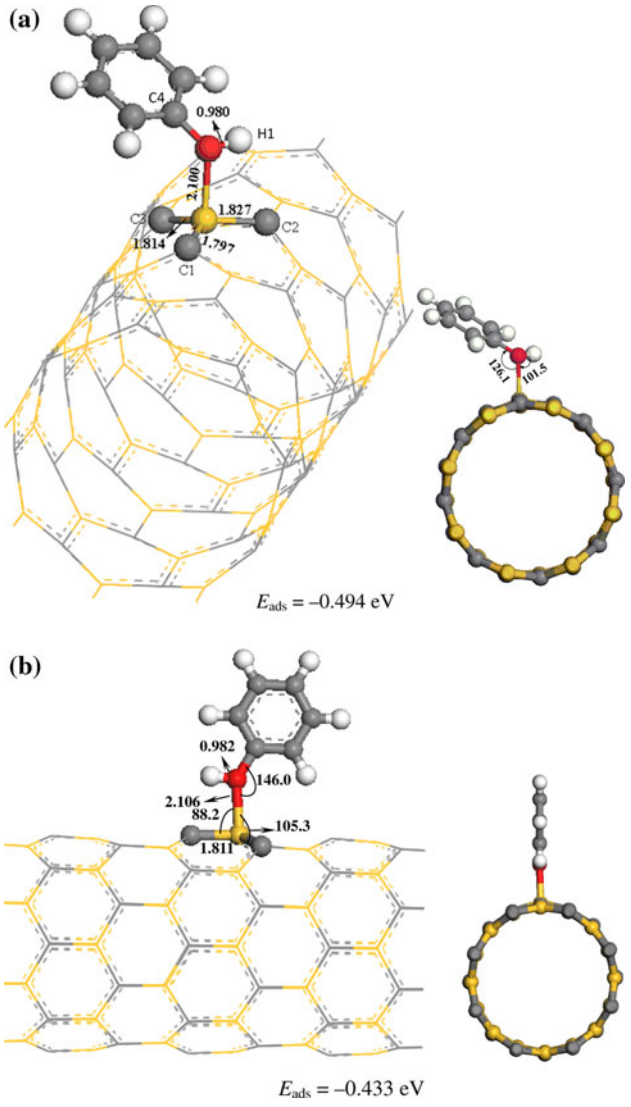

Fig. 1 The optimized structures of phenol adsorption on the SiCNT via the hydroxyl attacking. The aromatic ring of the phenol is (**a**) tilted and (**b**) vertical to the surface of the SiCNT. The bond distances and angles in angstroms and degrees, respectively

The synthesized silicon carbide nanotube (SiCNT) [36, 37] is a semiconducting material independent of its chirality. Due to its unique properties [38–48], SiCNT has been intensively studied. For example, SiCNT possesses good chemical reactivity and high stability at high temperatures, high power, and in harsh environments. These unique properties of the SiCNT might have great potential applications in many areas including gas sensors [49, 50], hydrogen storages [51], metal-free catalysts [52], and special (nano) optical devices [53, 54].

Inspired by the studies on the interaction between phenol and silicon surfaces, we are very interested in phenol adsorption on SiCNT surface in terms of the following reasons: (1) in terms of the semiconducting nature of the SiCNT, exploring phenol adsorption on SiCNT is helpful for the development of novel semiconductor-based hybrid materials; (2) SiCNT is shown to possess high reactivity, thus phenol might decompose on SiCNT surface, which initiates some catalytic reactions. Such issues might provide a useful guidance to develop SiCNT-based metal-free catalysts; (3) since both SiCNT and phenol molecule have unique structures and interesting properties, merging different branches of chemistry into a new avenue of research always generates great enthusiasm and interest among chemists. Unfortunately, to the best of our knowledge, there have been no reports on the study of phenol adsorption on the SiCNT. In this article, we have explored the adsorption of an isolated phenol molecule on the outer surface of the SiCNT using density functional theory (DFT) methods. In particular, the following issues will be considered: (a) since phenol is a bifunctional molecule, its two functional groups, the hydroxyl group and aromatic ring, might both interact with the SiCNT in various ways, the problem is which adsorption is more energetically favorable? (b) What are the effects of phenol adsorption on the electronic properties of the SiCNT?

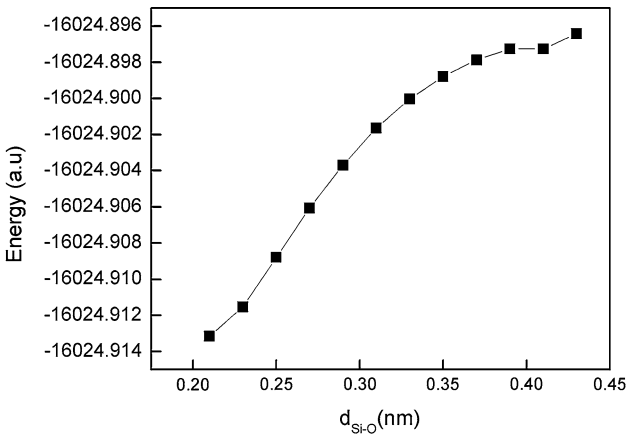

Fig. 2 The variation of the total energies of phenol–SiCNT with respect to the Si–O distance

2 Computational methods and models

We perform all-electron ab initio DFT calculations using double numerical basis set plus polarization functional (DNP basis set), which is implemented in the DMOL^3 package [55, 56]. The spin-polarized generalized gradient approximation (GGA) with the Perdew–Burke–Ernzerhof (PBE) [57] and the local density approximation (LDA) with the Perdew–Wang (PWC) functional [58] is used. Because the interaction between the SiCNT and the aromatic ring of phenol molecule might be physisorption in nature, we adopt both GGA and LDA to estimate the range of the adsorption energy. In fact, LDA has been shown to be a reliable functional to study the systems involving in the van der Waals interactions [59–61] and can give an adsorption energy much closer to the MP2 calculation [62–64]. This method has been successfully employed in the theoretical calculations of nanotube systems, including their functionalization [52, 65–69]. In the present work, GGA with the PBE method is utilized as the exchange–correlation functional throughout the paper. Moreover, a zigzag (8, 0) SiCNT with a diameter of 7.92 Å is adopted.

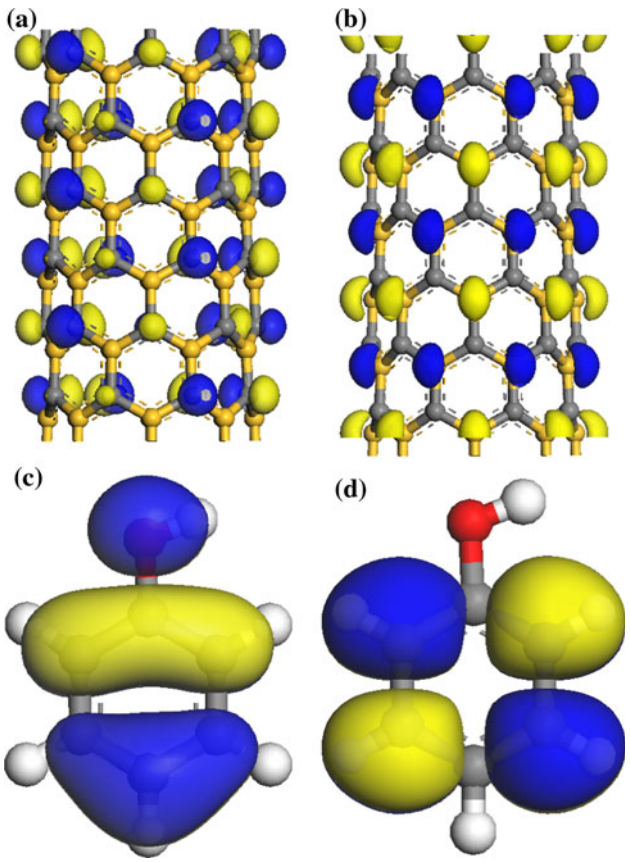

Fig. 3 The highest occupied molecular orbitals (HOMOs) and the lowest unoccupied molecular orbitals (LUMOs). **a** HOMOs and **b** LUMOs of the SiCNT, **c** HOMOs, and **d** LUMOs of the phenol molecule

This is because the stability of the single-walled SiCNT is diameter-dependent: SiCNT is more stable than the thinner faceted nanotube and nanowire [70]. However, as the diameter increases, nanowires and faceted nanotubes will be eventually more stable than SiCNTs [70]. The supercell with lattice constants of $a = b = 30$ Å and $c = 15.93$ Å for the (8, 0) SiC nanotube is adopted, which includes 48 Si atoms and 48 C atoms. The Brillouin zone is sampled by $1 \times 1 \times 5$ special k-points according to the Monkhorst–Pack scheme [71]. Moreover, band structures are computed with 21 k-points based on the most stable structures. This method can offer a reasonable balance between accuracy and computational resource. In addition, we use the linear/quadratic synchronous transit (LST/QST) method [72, 73] to calculate the transition states in this work.

3 Results and discussion

For the isolated phenol molecule, its optimized structural parameters are shown in Figure S1a of the supporting information, which are well consistent with previous reports [74, 75]. Because the phenol molecule has two functional groups (the hydroxyl group and aromatic ring), we consider two kinds of initial adsorption configurations for the bifunctional phenol on SiCNT: (a) hydroxyl-group-attacking and (b) aromatic-ring-attacking. In the former, the hydroxyl group is adsorbed on active sites of the SiCNT including the carbon (C), silicon (Si), and center hexagon (H) sites (Figure S1b). For the latter, however, the

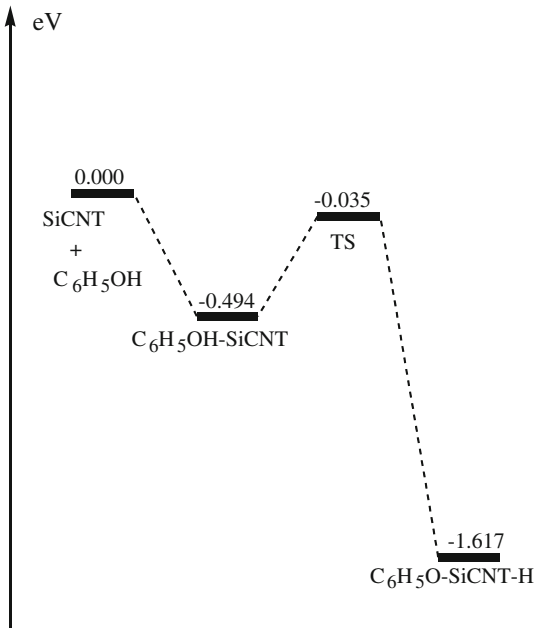

Fig. 4 Potential energy profiles for the O–H bond cleavage of the adsorbed phenol on the SiCNT

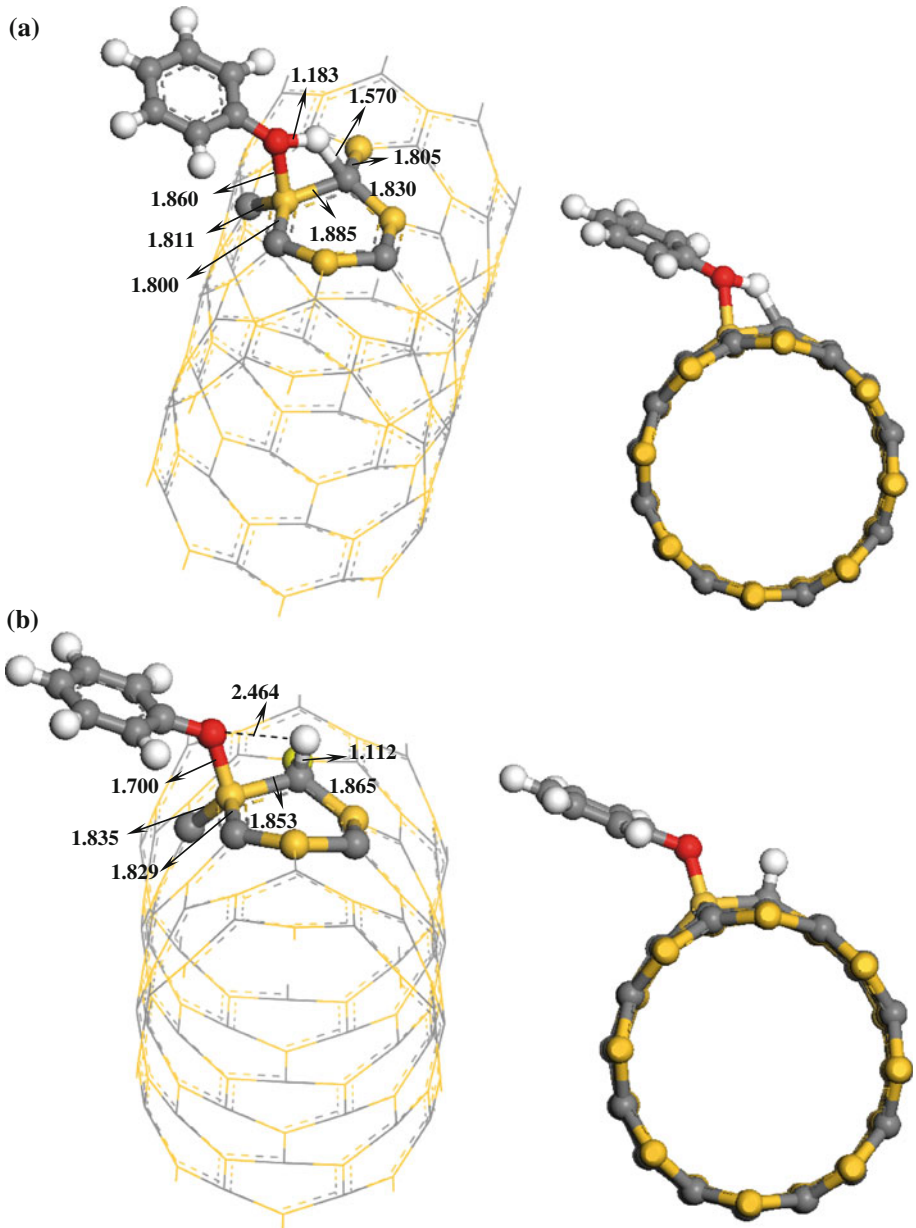

Fig. 5 The optimized structures of (**a**) transition state and (**b**) product complex of the O–H bond cleavage on the SiCNT. The bond distances in angstroms

aromatic ring of phenol lies in parallel above the hexagon of SiCNT via π–π interaction. We will discuss the two different kinds of phenol adsorption on the SiCNT in detail below.

3.1 Phenol adsorption on the SiCNT via the hydroxyl-group-attacking

First, we study phenol adsorption on the SiCNT by its hydroxyl group attacking toward the SiCNT. After structural optimizations, it is found that phenol adsorption on the C and H site is energetically unstable and is collapsed to the Si site, which is energetically favorable. In Fig. 1, we present two obtained stable structures and their corresponding adsorption energies. The most stable configuration is such that the oxygen atom of phenol is adsorbed on the Si atom of SiCNT, in which the aromatic ring of phenol is tilted to SiCNT as shown in Fig. 1a (labeled as tilted configuration). The adsorption energy of this configuration, which is defined as $E_{ads} = E_{total}(\text{SiCNT–phenol}) - E_{total}(\text{SiCNT}) - E_{total}(\text{phenol})$, is -0.494 eV, and about 0.208 electrons are transferred from phenol to SiCNT. Moreover, the distance between O atom of phenol and Si atom of SiCNT is about 2.100 Å. In addition, we plot the variation of the total energies of phenol–SiCNT with respect to the Si–O distance (Fig. 2). It is found that the total energies of phenol–SiCNT increase with the increase in the Si–O distance. Thus, phenol molecule can be adsorbed on the (8, 0) SiCNT barrierlessly. Similar to the covalent functionalization of carbon nanotubes [76] and boron nitride nanotubes [65–67, 77], phenol

adsorption can also induce apparent structural deformation to SiCNT, which pulls the adsorbed Si atom by phenol outwards the tube wall. The Si–C bond lengths in SiCNT involving in the adsorbed Si atom (1.797, 1.814, 1.827 Å) are longer than those in perfect SiCNT (1.780–1.800 Å) because the hybridization of the Si atom is transformed from sp^2 to sp^3 upon phenol adsorption.

As shown in Fig. 1b, a meta-stable configuration is also obtained, in which the O atom of the phenol molecule is bound with the Si atom of SiCNT, similar to the tilted-configuration (Fig. 1a). However, the aromatic ring of phenol in the meta-stable configuration is vertical to the surface of SiCNT (labeled as vertical-configuration). The distance between phenol and SiCNT is about 2.106 Å. For this configuration, the calculated adsorption energy and charge transfer from phenol to SiCNT are −0.433 eV and 0.155 e respectively, which are slightly weaker than those of the tilted configuration (−0.494 eV and 0.208 e). The adsorption of the hydroxyl group in phenol on the Si site in SiCNT can be rationalized by the fact that, in SiCNT, the highest occupied molecular orbitals (HOMOs Fig. 3a) are centered on the C sites, and the lowest unoccupied molecular orbitals (LUMOs Fig. 3b) are located on the Si sites. As a result, the HOMO of phenol (Fig. 3c) donates electrons preferably to the LUMO centered on the Si sites of SiCNT.

An attractive point for the phenol surface chemistry is that: some bond of phenol, e.g., O–H or C–O, might be split on solid surfaces, which can initiate many catalytic processes and thereby leads to the formation of a variety of useful products. Can the molecularly adsorbed phenol be also split on the (8, 0) SiCNT? On the basis of the above results, we further evaluate the possibility of bond cleavage of the molecularly adsorbed phenol on SiCNT. The results indicate that the O–H bond of the adsorbed phenol can be split barrierlessly, while the cleavage of the C–O bond cannot occur due to the large barrier and endothermicity. In Fig. 4, we list the process of the O–H bond cleavage on SiCNT.

Taking the tilted configuration (Fig. 1a) as an example, we elucidate the process of the O–H bond cleavage on SiCNT. After the molecular adsorption of phenol on SiCNT with the adsorption energy of −0.494 eV (Fig. 1a), we find that the H atom of the hydroxyl group of phenol is transferred from the Si atom to the neighboring C site through a transition state (Fig. 5a) with an intrinsic barrier of 0.459 eV. Moreover, the split product (C_6H_5O–SiC nanotube–H, Fig. 5b) lies at −1.617 eV with respect to the reactants (pure SiCNT and isolated phenol). Because the energy released by molecular adsorption of phenol on SiCNT (0.494 eV) is greater than the required H-transfer barrier (0.459 eV), we expected that the O–H bond of the adsorbed phenol can be easily split on SiCNT. Similar case can also be observed for the vertical configuration (Fig. 1b). The cleavage process, the involved transition state, and product were presented in Figure S2. We should point out that the singlet state is the ground state for the two split products, which is energetically lower by 1.169 (for tilted configuration) and 1.122 eV (vertical configuration), respectively. In addition, we also explore the cleavage of the C–O bond of the adsorbed phenol on SiCNT. It can be obviously seen from Figure S3, and this process is endothermic by 0.991 eV and the total barrier is as high as 2.021 eV. Therefore, the C–O bond cleavage of the adsorbed phenol on SiCNT cannot take place.

3.2 Phenol adsorption on SiCNT via the aromatic-ring-attacking

In this section, we focus on another phenol adsorption, i.e., phenol interacts with SiCNT via the π–π overlap. For this

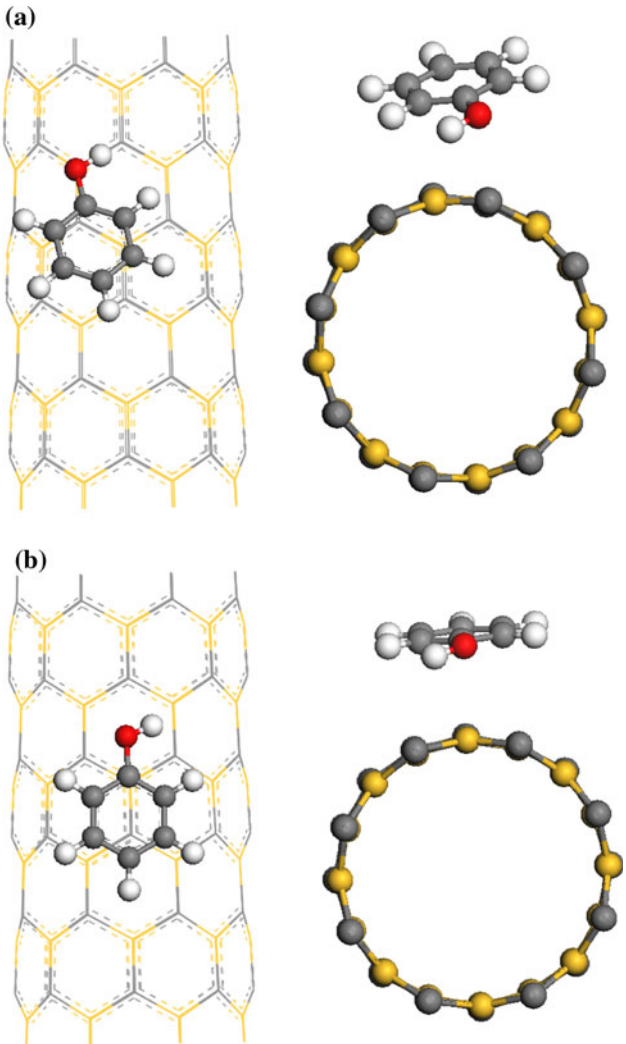

Fig. 6 The optimized structures of phenol adsorption on the (**a**) BZ site and (**b**) BA site of the SiCNT

kind of adsorption, phenol molecule is initially placed in parallel to the surface of SiCNT, thus the center of the aromatic ring located above a C, Si, BA, BZ, or H site in SiCNT as shown in Figure S4. After careful structural optimization, we find that phenol adsorption above C, Si, and H sites is collapsed to the BA and BZ sites, which are energetically favorable.

In Fig. 6, we list the two stable structures of the phenol above the BA and BZ sites of SiCNT. When comparing the two stable configurations, the phenol adsorption above the BZ site (Fig. 6a) is found to be more stable. The calculated E_{ads} is −0.285 eV, much weaker than that of the hydroxyl-group-attacking (−0.494 eV). The nearest distance between phenol and SiCNT is about 2.008 Å (the H atom of phenol is pointing to the Si atom of SiCNT). The small adsorption energy and the large distance indicate that this kind of adsorption is derived from the van der Waals (vdW) interaction. Furthermore, we note that the aromatic-ring-attacking configuration has a smaller adsorption energy (−0.383 eV) than that of the hydroxyl-group-attacking one (−0.926 eV) using LDA/PWC methods. In addition, this weak adsorption of the phenol on the

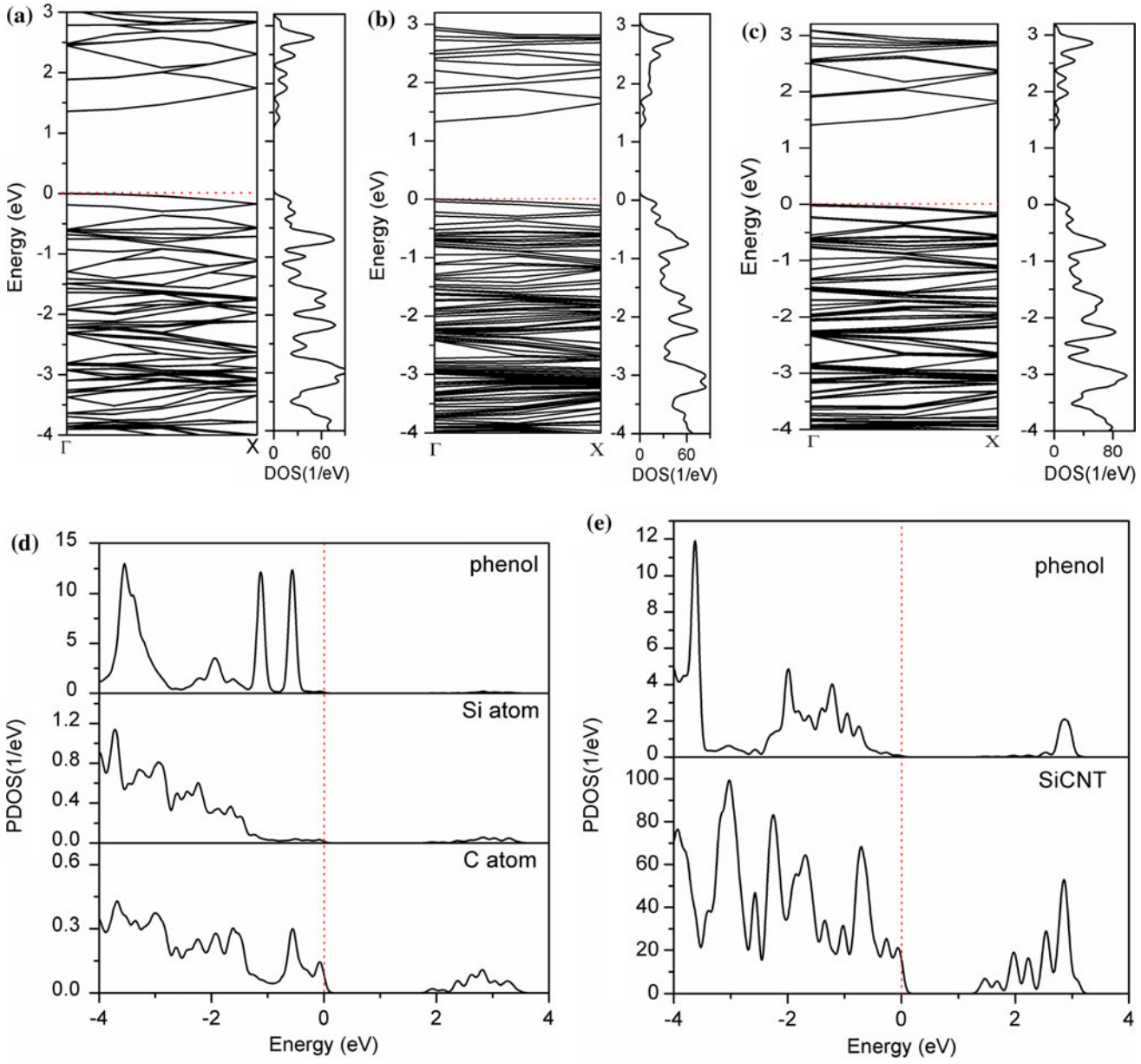

Fig. 7 The obtained band structures and density of states of (**a**) the pure SiCNT, the product complex of the (**b**) O–H bond cleavage, and (**c**) phenol adsorption via its aromatic ring. The projected DOS of the product complex of the (**d**) O–H bond cleavage and (**e**) phenol adsorption via its aromatic ring

SiCNT via the aromatic-ring-attacking is further testified by its neglectable charge transfer from the phenol to the SiCNT (0.064 eV). Moreover, when the aromatic ring of the phenol is adsorbed above the BA site of the SiCNT (Fig. 6b), the adsorption become slightly weaker ($E_{ads} = -0.125$ eV) when compared with the case of above the BZ site ($E_{ads} = -0.285$ eV).

3.3 The effects of phenol adsorption on the electronic properties of the SiCNT

To better understand phenol adsorption on SiCNT, we further study the changes in electronic properties of the adsorbed SiCNT by phenol. In Fig. 7, we present the calculated band structures and density of states (DOS) of SiCNT before and after phenol adsorption. The pure (8, 0) SiCNT has a band gap of 1.36 eV (Fig. 7a), which has a good agreement with previous reports [49, 59]. Upon adsorption of phenol molecule, we find that the electronic properties of SiCNT are little changed as shown in Fig. 7b and d: (1) the modified SiCNT is still a semiconductor; (2) the band gap and the band structures near the Fermi level are nearly unchanged, except that the band-structure symmetry of the pristine SiCNT is broken; (3) the total DOS and local projected DOS of phenol (Fig. 7c and d) show that the electronic states contributed from phenol molecule are far away from the Fermi level.

In short, when phenol molecule is adsorbed on SiCNT, it is favorable to be adsorbed on the nanotube with its hydroxyl group. Because the energy released by molecular adsorption of phenol on SiCNT (0.494 eV) is greater than the required H-transfer barrier (0.459 eV), we expected that the O–H bond of the adsorbed phenol can be easily split on SiCNT. Conversely, to remove the decomposed phenol from the SiCNT sidewall, a large energy barrier of $\sim$1.582 eV has to be overcome, suggesting that the C_6H_5O–SiCNT–H system is very stable at room temperature.

4 Conclusion

By performing density functional theory calculations, we have studied phenol adsorption on an (8, 0) SiCNT. Two different kinds of phenol adsorption have been considered; i.e., (1) the hydroxyl group and (2) aromatic ring attack the SiCNT, respectively. For the former, we find that the O–H bond of phenol dissociates on the SiCNT via a two-step mechanism: (a) phenol is molecularly adsorbed on the SiCNT ($E_{ads} = -0.494$ eV), followed by (b) the O–H bond of adsorbed phenol is split with an intrinsic barrier of 0.459 eV. Considering that the exothermicity (0.494 eV) in the first step is larger than the barrier of H transfer in the second step (0.459 eV), we expect that the cleavage of O–H bond of phenol on the SiCNT occur easily, which is very useful to initiate some catalytic reactions. Moreover, phenol adsorption using its aromatic ring on SiCNT via π–π interaction is shown to be weak with adsorption energy of -0.285 eV. Additionally, the calculated band structures and DOS suggest that the electronic properties of SiCNT are little changed after adsorption of phenol. The present results not only are useful to the verification of the good chemical reactivity of SiCNT but also provide an effective way for the transformation or removal of phenol.

Acknowledgments This work is supported by the Committee of Education of Heilongjiang Province (11541095), the Natural Science Foundation of Heilongjiang Province (ZD200820-01, B200814), and the Key Project of Chinese Ministry of Education. (NO. 210060). The authors would like to show great gratitude to the reviewers for raising invaluable comments and suggestions.

References

1. Ma Z, Zaera F (2006) Surf Sci Rep 61:229
2. Tao F, Bernasek SL, Xu GQ (2009) Chem Rev 109:3991
3. Jenkins SJ (2009) Proc R Soc A 465:2949
4. Zhuang SX (1996) Chin Chem Lett 7:661
5. Lu L, Salaita GN, Laguren-Davidson L, Stern DA, Wellner E, Frank DG, Batina N, Zapien DC, Walton N, Hubbard AT (1988) Langmuir 4:637
6. Bu H, Bertrand P, Rabalais JW (1993) J Chem Phys 98:5855
7. Guo XC, Madix RJ (1995) Surf Sci 341:L1065
8. Steinmüller D, Ramsey MG, Netzer FP (1992) Surf Sci 271:567
9. Liu AC, Friend CM (1990) Surf Sci Lett 236:L349
10. Ramsey MG, Rosina G, Steinmüller D, Graen HH, Netzer FP (1990) Surf Sci 232:266
11. Richardson NV, Hofmann P (1983) Vacuum 33:793
12. Solomon JL, Madix RJ, Stohr J (1991) Surf Sci 255:12
13. Carbone M, Piancastelli MN, Casaletto MP, Zanoni R, Besnard-Ramage MJ, Comtet G, Dujardin G, Hellner L (1999) Surf Sci 419:114
14. Ihm H, White JM (2000) J Phys Chem B 104:6202
15. Xu X, Friend CM (1989) J Phys Chem 93:8072
16. Russell JN, Sarvis SS, Morris RE (1995) Surf Sci 338:189
17. Serafin JG, Friend CM (1989) Surf Sci 209:L163
18. Russell JN, Leming A, Morris RE (1998) Surf Sci 399:239
19. Bartlett B, Valdisera JM, Russell JN (1999) Surf Sci 442:265
20. Myers AK, Benziger JB (1989) Langmuir 5:127
21. Wallace J, Kirk-Othmer (2005) Encyclopedia of chemical technology, vol 18, 3rd edn. p 747
22. Chakarova SD, Carlsson AE (2004) Phys Rev E 69:021907
23. Lopinski G, Wayner D, Wolkow R (2000) Nature 406:48
24. Besley NA, Blundy AJ (2006) J Phys Chem B 110:1701
25. Quek SY, Neaton JB, Hybertsen MS, Kaxiras E, Louie SG (2006) Phys Status Solid B 243:2048
26. Casaletto MP, Carbone M, Piancastelli MN, Horn K, Weiss K, Zanoni R (2005) Surf Sci 582:42
27. Busca G, Berardinelli S, Resini C, Arrighi L (2008) J Hazard Mater 160:265
28. Delle Site L, Alavi A, Abrams CF (2008) Phys Rev B 67:193406
29. Ghiringhelli LM, Caputo R, Delle Site L (2007) Phys Rev B 75:113403

30. Jayanthi N, Cruz J, Pandiyan T (2008) Chem Phys Lett 455:64
31. Salo P, Blomqvist J (2009) J Phys: Condens Matter 21:225001
32. Marilena C, Simone M, Ruggero C (2007) Phys Rev B 76:085332
33. Karen J, Andris G, Tuukka V, Martti JP (2010) Phys Rev B 81:235428
34. Bertoncini C, Odetti H, Bottani EJ (2000) Langmuir 16:7457
35. Chakarova-Käck SD, Borck Ø, Schröder E, Lundqvist BI (2006) Phys Rev B 74:155402
36. Sun XH, Li CP, Wong WK, Wong NB, Lee CS, Lee ST, Teo BK (2002) J Am Chem Soc 124:14464
37. Pham-Huu C, Keller N, Ehret G, Ledouxi MJ (2001) J Catal 200:400
38. Fan JY, Wu XL, Paul KC (2006) Prog Mater Sci 51:983
39. Melinon P, Masenelli B, Tournus F, Perez A (2007) Nat Mater 6:479
40. Teo BK, Sun XH (2007) Chem Rev 107:1454
41. Teo BK, Huang SP, Zhang RQ, Li WK (2009) Coordin Chem Rev 253:2935
42. Menon M, Richter E, Andriotis AN (2004) Phys Rev B 69:115322
43. Zhao M, Xia Y, Li F, Zhang RQ, Lee ST (2005) Phys Rev B 71:085312
44. Patrick AD, Dong X, Allison TC, Barojas EB (2009) J Chem Phys 130:244704
45. Wang Z, Gao F, Li J, Zu X, Weber WJ (2009) Nanotechnology 20:075708
46. Zhang JM, Chen LY, Wang SF, Xu KW (2010) Eur Phys J B 73:555
47. Yu M, Jayanthi CS, Wu SY (2010) Phys Rev B 82:075407
48. Alam KM, Ray AK (2008) Phys Rev B 77:035436
49. Zhao JX, Ding YH (2009) J Chem Theory Comput 5:1099
50. Wu RQ, Yang M, Lu YH, Feng YP, Huang ZG, Wu QY (2008) J Phys Chem C 112:15985
51. Mpourmpakis G, Froudakis GE, Lithoxoos GP, Samios J (2006) Nano Lett 6:1581
52. Zhao JX, Xiao B, Ding YH (2009) J Phys Chem C 113:16736
53. Wang L, Lu J, Luo GF, Song W, Lai L, Jing MW, Qin R, Zhou J, Gao ZX, Mei WN (2007) J Phys Chem C 111:18864
54. Wu IJ, Guo GY (2007) Phys Rev B 76:035343
55. Delley B (1990) J Chem Phys 92:508
56. Delley B (2000) J Chem Phys 113:7756
57. Perdew JP, Burke K, Ernzerhof M (1996) Phys Rev Lett 77:3865
58. Perdew JP, Wang Y (1992) Phys Rev B 45:13244
59. Cobian M, Iniguez J (2008) J Phys Condens Matter 20:285212
60. Ataca C, Aktürk E, Ciraci S, Ustunel H (2008) Appl Phys Lett 93:043123
61. de Andres PL, Ramírez R, Vergés JA (2008) Phys Rev B 77:045403
62. Cabria I, López MJ, Alonso JA (2005) J Chem Phys 123:204721
63. Okamoto Y, Miyamoto Y (2001) J Phys Chem B 105:3470
64. Wu XJ, Gao Y, Zeng XC (2008) J Phys Chem C 112:8458
65. Wu XJ, Yang JL, Zeng XC (2006) J Chem Phys 125:044704
66. Wu XJ, Yang JL, Zeng XC (2006) J Chem Phys 125:044711
67. Wu XJ, An W, Zeng XC (2006) J Am Chem Soc 128:12001
68. Zhao JX, Ding YH (2008) J Phys Chem C 112:2558
69. Zhao JX, Ding YH, Cai QH, Wang XG, Wang XZ (2010) J Phys Chem C 114:3825
70. Li YF, Zhou Z, Chen YS, Chen ZF (2009) J Chem Phys 130:204706
71. Monkhorst HJ, Pack JD (1976) Phys Rev B 13:5188
72. Henkelman G, Jonsson H (2000) J Chem Phys 113:9978
73. Olsen RA, Kroes GJ, Henkelman G, Arnaldsson A, Jonsson H (2004) J Chem Phys 121:9776
74. NIST Computational Chemistry Comparison, Benchmark Database, NIST Standard Reference Database Number 101, Release 12, Aug (2005) In: Russell D Johnson III (ed) http://srdata.nist.gov/cccbdb
75. Larsen NW (1979) J Mol Struct 51:175
76. Zhao JJ, Park H, Han J, Lu JP (2004) J Phys Chem B 108:4227
77. Li YF, Zhou Z, Zhao JJ (2007) J Chem Phys 127:184705